JOURNAL OF GUIDANCE, CONTROL, AND DYNAMICS
Vol. 22, No. 2, March–April 1999

Robust Integrated Flight and Propulsion Controller for the Harrier Aircraft

Ian Postlethwaite* and Declan G. Bates†
Leicester University, Leicester, England LE1 7RH, United Kingdom

An integrated longitudinal plus lateral flight and propulsion control system is designed for the Harrier short takeoff and vertical landing aircraft, using the technique of $\mathcal{H}_\infty$ loop shaping. This centralized controller is partitioned via a step by step procedure, which generates both nominal performance and robust stability specifications for the engine subsystem. Performance properties of both the centralized and partitioned systems are validated via nonlinear simulation. Implications of the design experience for the implementation of a full integrated flight and propulsion control system on the Harrier are considered.

Nomenclature

E	= error signals
$etad$	= tailplane deflection, deg
fnp	= engine fan speed, rpm
$G(s)$	= plant transfer function matrix
hnp	= compressor speed, rpm
$K(s)$	= $\mathcal{H}_\infty$ loop-shaping controller
p	= roll rate, rad/s
$pthtp$	= throttle position, dimensionless
q	= pitch rate, rad/s
qef	= fuel flow, gal/h
r	= yaw rate, rad/s
$thejd$	= nozzle angle, deg
U	= control inputs
vd	= velocity down, ft/s
ve	= velocity east, ft/s
vf	= velocity forward, ft/s
$vtkt$	= total airspeed, kn
xid	= aileron deflection, deg
Z	= controlled variables
$zetad$	= rudder deflection, deg
α	= angle of attack, deg
β	= angle of sideslip, deg
γ	= flight-path angle, climb, deg
θ	= pitch attitude, rad
$\bar{\sigma}$	= maximum singular value
ϕ	= roll attitude, rad
ψ	= yaw attitude, rad

Subscripts

a, e	= airframe subsystem, engine subsystem
c	= command value
ea	= interface from engine subsystem to airframe subsystem

I. Introduction

RESULTS are presented from the first phase of a program of research carried out by the authors for the Defence and Evaluation Research Agency (DERA), on the design of an integrated flight and propulsion control system for the vectored thrust aircraft advanced flight control (VAAC) Harrier aircraft. The VAAC aircraft is a short takeoff and vertical landing (STOVL) Harrier T4 two-seater trainer, which has been fitted with an experimental digital flight control system, designed to permit flight testing of experimental flight control laws. VAAC is a U.K. Ministry of Defence program with the objectives of flight demonstration of advanced vertical or short takeoff and landing (V/STOL) flight controls and handling qualities assessment techniques. Under this program several experimental control laws for the Harrier have been developed for the DERA,[1] and these designs have been evaluated both on the full motion piloted simulation facilities at DERA Bedford and in flight tests. Also, in Refs. 2 and 3, successful flight tests are reported for experimental control laws for the Harrier, designed using modern multivariable techniques. These control laws have, however, not attempted to fully integrate the flight and propulsion control systems and have, in general, been restricted to controlling the longitudinal motion of the aircraft.

The aim of the first phase of the project carried out at Leicester University for the DERA was to develop a systematic methodology for integrated flight and propulsion control (IFPC) system design for the Harrier, using multivariable robust controller design techniques. Preliminary results from the project have been presented in Refs. 4 and 5. In this paper details are given of the application in nonlinear simulation of the developed IFPC methodology to the VAAC Harrier aircraft in the 80-kn transition flight phase.

A significant advance in aerospace engineering in recent years has seen the development of actuator technologies that allow much greater flexibility in the use of propulsion generated thrusts as primary flight control effectors. Pitch, roll, and yaw moments necessary for attitude control, as well as various thrust and lift forces necessary for trim and maneuvering control, can now all be partially or exclusively generated by vectoring nozzles and various propulsive lift systems such as ejectors, remote augmented lift systems, and various techniques of boundary-layer control using engine air.[6] The development of these new technologies means that there are now many combinations of aerodynamic and propulsion effectors that can be employed to enhance control authority during STOVL and conventional operations, to minimize fuel consumption and pilot workload throughout different flight modes and to permit reconfiguration in the event of malfunction of one or more components. The use of propulsion effectors for aerodynamic control creates significant interaction between the two (heretofore independent) subsystems, necessitating a multivariable, robust approach to IFPC design.

In Refs. 7 and 8 a methodology for IFPC design was developed, based on a centralized approach to the problem. This approach consists of first designing a centralized controller considering the airframe and propulsion subsystems as one integrated system and then partitioning the centralized controller into decentralized independent subcontrollers with a specified coupling structure. The subcontrollers will, in general, be of lower order than the centralized controller and will, thus, be easier to implement. They can also be independently tested and validated at subsystem level. Independent integrity of the subcontrollers is necessary not just for control theoretic reasons (different types of control to be applied to

Received Nov. 3, 1997; revision received July 1, 1998; presented as Paper 98-4295 at the AIAA Guidance, Navigation, and Control Conference, Boston, MA, Aug. 10–12, 1998; accepted for publication Sept. 26, 1998.

*Professor, Control Systems Research, Department of Engineering.
†Lecturer, Control Systems Research, Department of Engineering.

systems with different dynamics, uncertainties, nonlinearities, etc.) but for practical and political reasons as well. Because different subsystems may be designed and built by different and independent suppliers, design accountability and commercial issues will often dictate that each manufacturer retains a high degree of control over the particular subsystem (and its controller) for which it is responsible.

This study investigates the application of the $\mathcal{H}_\infty$ loop-shaping design method to the VAAC Harrier IFPC problem, under the general framework for IFPC system design detailed in Ref. 7. The objectives of the paper are the evaluation of the $\mathcal{H}_\infty$ loop-shaping design method as a candidate technique for centralized controller design and the formulation of a systematic methodology for IFPC design for the Harrier STOVL aircraft.

The layout of the paper is as follows. Section II introduces the VAAC Harrier IFPC problem addressed in this study. Section III details the design of a centralized $\mathcal{H}_\infty$ loop-shaping controller for this problem. In Sec. IV, the centralized controller is partitioned via a modified version of the procedure detailed in Ref. 9. The modifications to the partitioning procedure are necessary due to the nature of the control problem addressed, as well as to the particular implementation structure chosen for the $\mathcal{H}_\infty$ loop-shaping controller. Some additional robustness specifications for the partitioned controller are developed. Section V contains a discussion of the approach to IFPC design adopted in this study, and Sec. VI offers some conclusions.

II. VAAC Harrier IFPC Problem

The aircraft model used in this study is the Harrier wide envelope model (WEM): a full envelope nonlinear lateral plus longitudinal representation of the aerodynamics, engine, and actuator characteristics of the VAAC Harrier aircraft. The WEM software incorporates a full thermodynamic powerplant simulation of a Pegasus engine, which is integrated with the airframe system dynamics: thus, in principle, all interactions between these two systems are captured in this model. Representative actuation systems, including rate and saturation limits, have been placed on all control motivators. Saturation limits for control motivators are as follows: *etad*: −10.25–11.25 deg, *xid*: ±14 deg, *zetad*: ±15 deg, *thejd*: 0–98.5 deg, and *pthtp*: 0.26–1. The WEM software is coded in Fortran and run under the SIMULINK[10] simulation environment. The overall software package represents a highly detailed model of the aircraft, producing 22 aerodynamic outputs and 12 engine outputs. The package was configured to allow the extraction of linear state-space models at various points over the flight envelope for the purposes of control system design. These (lower-order) linear models are of the form

$$\dot{\boldsymbol{x}} = A\boldsymbol{x} + B\boldsymbol{u}, \qquad \boldsymbol{y} = C\boldsymbol{x} + D\boldsymbol{u}$$

where the state vector and control inputs are given by

$$\boldsymbol{x} = [\theta, \phi, \psi, q, p, r, vf, ve, vd, fnp, hnp, qef]$$

$$\boldsymbol{u} = [etad, xid, zetad, thejd, pthtp]$$

All of the states just defined are available as outputs. Both the linear and nonlinear WEM models cover the full flight envelope for the VAAC, from fully airborne flight at 200 kn down to hover. Details of a centralized IFPC design carried out at the 150-kn point of the flight envelope can be found in Ref. 5. In this paper, the linear model corresponding to the 80-kn transition flight phase from fully airborne flight to hover is used for controller design. At this point in the flight envelope, the aircraft is longitudinally unstable and propulsion system generated forces and moments are taking over control of the aircraft from the aerodynamic effectors. The controlled variables z are given by

$$\boldsymbol{z} = [Qq, Pp, r, vf, vd]$$

where $Qq = q + 0.3\theta$, $Pp = p + 0.3\phi$, and the others are as earlier defined. The given choice of controlled variables was based on control configuration mode 4 of the NASA V/STOL systems research aircraft.[11] The choice of Qq and Pp corresponds to designing a rate command-attitude hold system and provides response types that are generally desirable for good handling qualities in transition flight.[8] Performance specifications, based on Ref. 12, for the closed-loop system are given as follows.

1) For the pitch, roll, and yaw outputs, 90% of demanded rate/attitude to be reached within 2 s.

2) Bandwidth of the pitch, roll, and yaw channels to be approximately 7 rad/s.

3) Within 4 s 90% of demanded velocity to be reached.

4) Maximize decoupling of command tracking over all channels, ensuring: a) 10-deg attitude demand causes less than 1-deg change in other attitudes and less than 1-kn change in velocities and b) 10-kn velocity demand causes less than 1-kn change in other velocities and less than 1 deg change in attitudes.

5) Control signals to stay within rate/saturation limits at all times.

No engine variables have been included in the vector of controlled variables z, due to the limited number of control inputs available on the linear model of the Pegasus engine used in this design. The methodology detailed in this paper has been developed to be as independent as possible of specific aircraft configurations, however, and therefore automatically allows the option of directly controlling engine variables in both the centralized and partitioned control schemes. This capability will be required for the next phase of the project, which will apply the IFPC methodology to a new model of the VAAC Harrier with a detailed thermodynamic representation of a Rolls Royce Spey turbofan engine. The new integrated model makes provision for thrust split demands and the use of inlet guide vanes and variable nozzle area as internal control variables and will, thus, allow direct control of key engine variables, as well as more complex partitioning arrangements.

III. Robust Centralized IFPCS Design

The controller design methodology used in this study is the $\mathcal{H}_\infty$ loop-shaping procedure of McFarlane and Glover.[13] Certain advantages of this method over traditional mixed sensitivity $\mathcal{H}_\infty$ optimization are now well documented in the literature.[3,14] As noted in Ref. 7, a key requirement for IFPC design is that the synthesis procedure be capable of capturing the very different performance requirements of aerodynamic flight control and aeroengine control. The successful application of $\mathcal{H}_\infty$ loop shaping to real industrial flight control and aeroengine control problems,[3,15] thus, makes it an obvious candidate. Furthermore, various studies carried out by British Aerospace on full-authority fly-by-wire control systems, summarized in Ref. 3, have indicated that separating the design into the two steps of 1) command feedforward design and 2) robust closed-loop stabilization results in a very effective design approach, which easily arrives at good handling qualities combined with good stability margins. This is exactly the approach adopted in the method of $\mathcal{H}_\infty$ loop shaping. The structure of the closed-loop system with a one-degree-of-freedom $\mathcal{H}_\infty$ loop-shaping controller $K(s)$ is shown in Fig. 1. The design parameters in the $\mathcal{H}_\infty$ loop-shaping procedure are the transfer function matrix W_1 and the two constant matrices W_2 and k. All three matrices are, in general, diagonal. An essential initial step in the design procedure is the proper scaling of the plant inputs and outputs.[16] In this example, input scaling was applied to the plant to normalize the actuator signals by their maximum allowable values. Cross coupling between all outputs was considered of equal importance, and so output scaling was used only to convert the units of the first three outputs from radians to degrees. Note that the scaled plant $G(s)$ in this example also includes linearized models of the dynamics of the plant actuators. The design procedure itself then consists of two basic steps. First, the weighting matrices W_1, W_2, and k are chosen to shape the singular values of the open-loop plant

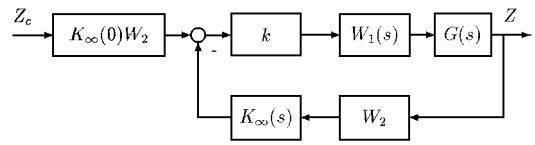

Fig. 1 Implementation structure of the $\mathcal{H}_\infty$ loop-shaping controller $K(s)$.

so that the given performance specifications are satisfied. Then, the feedback controller $K_\infty(s)$ is calculated so that the shaped plant is robustly stabilized against normalized coprime factor uncertainty. For this example, the weighting matrices were chosen as

$$W_1(s) = [(s+5)/s]I_{5\times 5}, \qquad W_2 = I_{5\times 5}$$

$$k = \text{diag}\,[0.1 \quad 0.2 \quad 0.1 \quad 0.15 \quad 0.1]$$

W_1 was chosen to ensure good tracking properties with zero steady-state error, good disturbance rejection at low frequencies, and a moderate rolloff rate around crossover. The matrix W_2 is generally used to reflect the relative importance of the outputs to be controlled and was, therefore, chosen as the identity matrix for this example. Finally, the matrix k was used to set the bandwidth of the open-loop singular values and to adjust the relative magnitudes of the various actuator signals. The implementation structure shown in Fig. 1 has the advantage that reference signals do not directly excite the dynamics of $K_\infty(s)$; because this block has been designed for stabilization and not performance purposes, its presence in the forward loop can result in large amounts of overshoot (classical derivative kick). The constant prefilter $K_\infty(0)W_2$ is included to ensure zero steady-state tracking error, assuming integral action in W_1. The second step in the design procedure is the calculation of the $\mathcal{H}_\infty$ robust stabilization controller $K_\infty(s)$. Unlike with standard $\mathcal{H}_\infty$ optimization, no γ-iteration-type procedures are necessary for this calculation, which only involves the solution of two Riccati equations. Once $K_\infty(s)$ has been calculated, a stability margin function[13] $\epsilon_{\max}$ gives a measure of the amount of coprime factor uncertainty that can be tolerated before the closed-loop system goes unstable. For $\epsilon_{\max} > 0.25$, i.e., allowable coprime factor uncertainty of $>25\%$, it can be shown theoretically[13] that the controller $K_\infty(s)$ does not significantly change the shapes of the open-loop singular values. Thus, robust stabililty is achieved without significant degradation in performance characteristics. If $\epsilon_{\max}$ is less than 0.25, this indicates that the chosen loop shapes are incompatible with robust stability, and further adjustement of the weighting functions is then required. For this example, a robust stabilization controller $K_\infty(s)$ was calculated with an $\epsilon_{\max}$ of 0.3.

The performance of the linear $\mathcal{H}_\infty$ loop-shaping controller $K(s)$ was evaluated on the nonlinear WEM software model in time-domain simulations. Figure 2 shows the responses of the longitudinal controlled variables for a demand of 20 kn in forward velocity. Figure 3 gives the corresponding control signals. No significant coupling was observed between longitudinal and lateral responses. Figure 4 shows responses for a demand in Pp corresponding to a 16-deg change in ϕ. The responses are seen to meet command tracking, decoupling, and control usage specifications. Similar performance was observed for demands on the other controlled variables; further simulation results are given in Refs. 4 and 5.

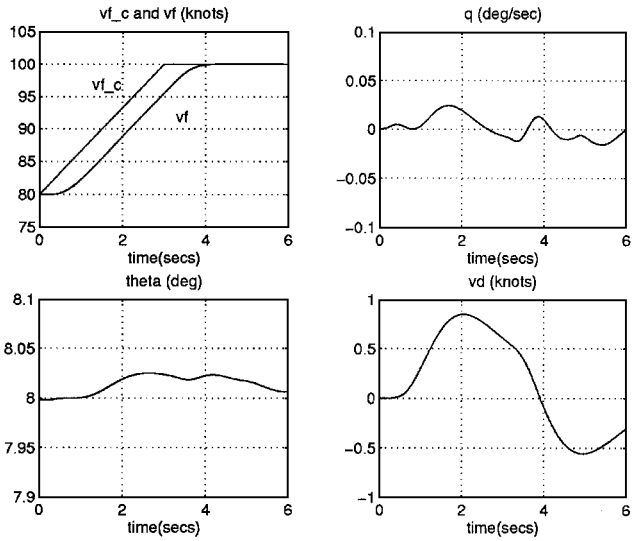

Fig. 2 Nonlinear responses for *vf* demand, centralized controller.

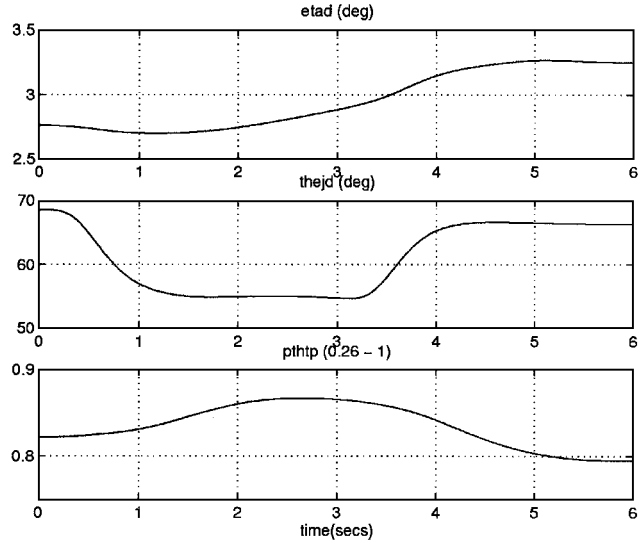

Fig. 3 Control signals for *vf* demand, centralized controller.

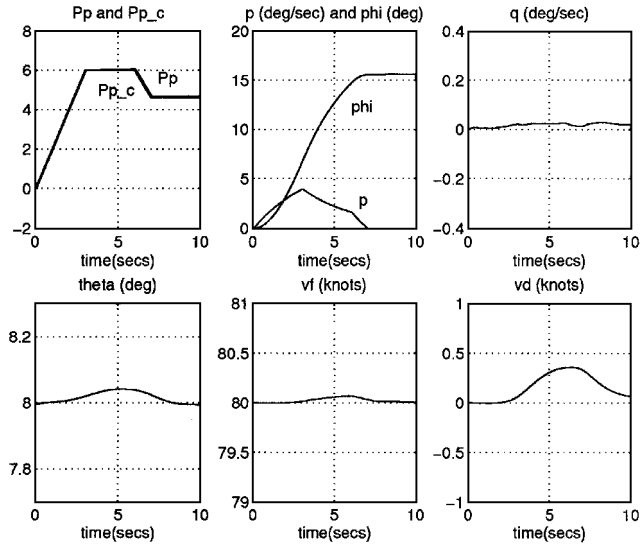

Fig. 4 Nonlinear responses for *Pp* demand, centralized controller.

IV. Centralized Controller Partitioning

The controller partitioning procedure adopted is based on that presented in Ref. 9, with appropriate modifications arising from 1) the particular implementation structure of $\mathcal{H}_\infty$ loop-shaping controllers and 2) the nature of the design problem considered. In the following, the dependence of the subcontroller blocks on frequency is suppressed in the notation for the sake of clarity. The steps in the procedure can be summarized as follows:

1) Separate the outputs of the plant into engine controlled variables Z_e, airframe controlled variables Z_a, and interface variables Z_{ea} and Z_{ae}. This step identifies which variables affect only the dynamics of their own subsystems (Z_e and Z_a) and which are responsible for interactions between subsystems (Z_{ea} and Z_{ae}). For this design no engine variables are included in the vector of controlled variables Z, and thus Z_e is empty, and all engine variables can be considered as interface variables Z_{ea}. The effect of airframe variables on engine variables is assumed negligable, and therefore Z_{ae} can also be set to zero. Thus,

$$Z_a = Z, \qquad Z_{ea} = [fnp, hnp, qef], \qquad Z_e = 0, \qquad Z_{ae} = 0$$

2) Separate the control effectors into engine U_e and airframe U_a inputs based on control effectiveness studies. In this design

$$U_a = [etad, xid, zetad, thejd], \qquad U_e = [pthtp]$$

Although the nozzle angle $thejd$ is part of the propulsion subsystem, it is included in U_a because it directly affects aircraft velocities, attitudes, and rates.

3) Under the assumption that subsystem interaction is in one direction only, i.e., from engine variables to airframe variables, the engine subcontroller K_{ee} can be calculated directly from the centralized $\mathcal{H}_\infty$ loop-shaping controller $K(s)$. Considering $K(s)$ as a transfer function matrix, K_{ee} is given as the portion of this matrix with inputs $E_e = Z_{ec} - Z_e$ and outputs U_e. Note that for the design example under consideration this step can be skipped because Z_e has been set to zero.

4) Generate specifications for the interface variables Z_{ea} from inspection of the closed-loop response from Z_{ac} to Z_{ea} with the centralized controller.

This step identifies the dynamic response that must be achieved by the interface subcontroller for the performance of the partitioned system to match that achieved with the centralized controller. From inspection of the relevant responses, it was decided that the interface controller K_{ea} should have a closed-loop bandwidth of 30 rad/s with zero steady-state tracking error. Note that this represents a nominal performance specification for the interface subcontroller.

5) Calculate an interface subcontroller K_{ea} to satisfy the specifications. Because the number of outputs is greater than the number of control inputs, independent control of all of the interface variables is not possible. Selection of qef as the output to be controlled directly, however, allowed the design of an $\mathcal{H}_\infty$ loop-shaping controller that met all of the derived specifications. The design parameters for this controller are given as

$$k_{\text{ea}} = 0.01, \qquad W_{1\text{ea}} = (s+2)/s, \qquad W_{2\text{ea}} = 1$$

6) Calculate the airframe subcontroller block K_a as a reduced-order approximation of the E_a to $[U_a \;\; Z_{\text{ea}}]$ transfer function matrix with the centralized controller, see Fig. 5.

For this design the complete airframe subcontroller is then made up of K_a together with the $K_\infty(s)$, W_2, and $K_\infty(0)W_2$ blocks from the centralized controller. The structure of the partitioned integrated controller is shown in Fig. 6. The centralized $\mathcal{H}_\infty$ loop-shaping controller has been replaced by independent airframe and engine subcontrollers with a specific interconnection structure. In this way the partitioned IFPC system improves the overall transparency of the design and also provides insight into the effects of lowering the order of each subsystem block on the performance of the overall system. The controller order reduction technique chosen for this study is the method of balanced residualization.[17] In this approach, the states of the balanced system with small Hankel singular values are residualized as opposed to truncated, thus retaining more information about the original system as well as preserving the dc gain. Application of this technique to the partitioned system reduced the orders of the K_a and $K_\infty(s)$ blocks of the airframe subcontroller from 10 to 9

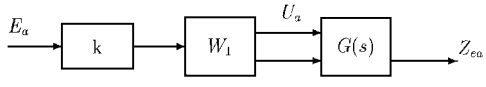

Fig. 5 Calculation of K_a block of airframe subcontroller.

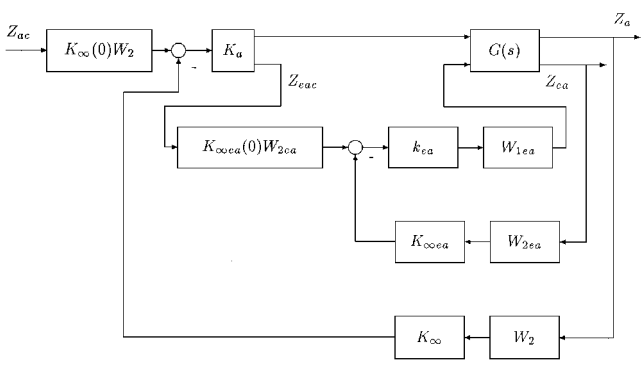

Fig. 6 Partitioned $\mathcal{H}_\infty$ loop-shaping controller.

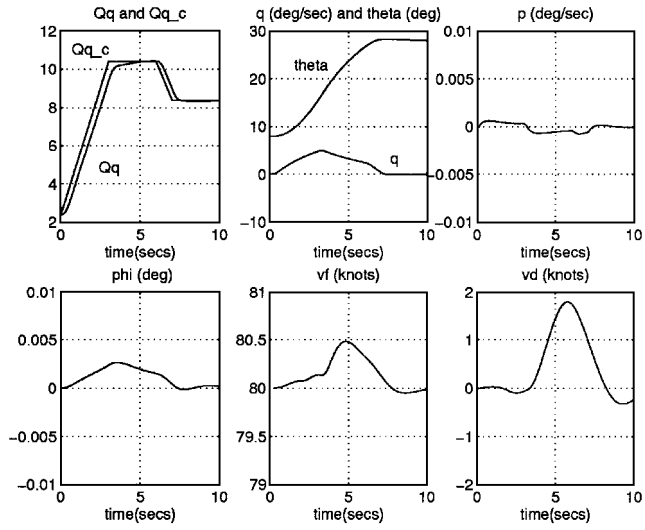

Fig. 7 Nonlinear responses for Qq demand, partitioned system.

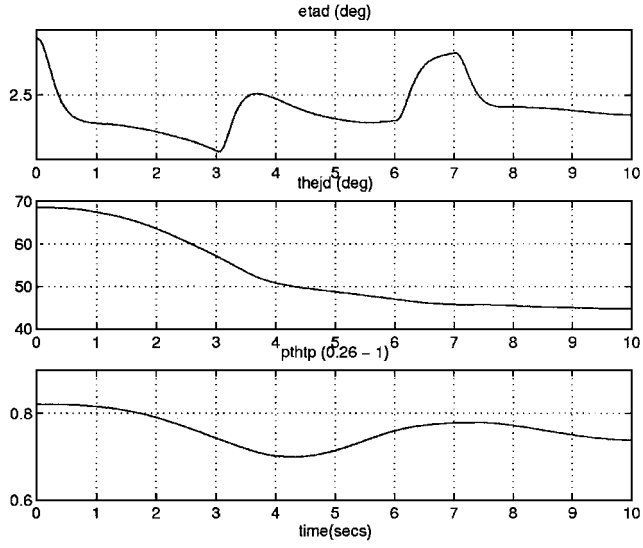

Fig. 8 Control signals for Qq demand, partitioned system.

and from 27 to 17, respectively. The order of the $K_{\infty\text{ea}}$ block of the engine subcontroller was reduced from 6 to 2. The reduced-order partitioned IFPC system was again evaluated in nonlinear simulation. Responses of the longitudinal controlled variables and the control signals to a demand in Qq are given in Figs. 7 and 8, respectively. As with the centralized design, there was no significant coupling between longitudinal and lateral axes. Responses were in general slightly slower but continued to meet the specifications. Further simulation results are given in Ref. 4. Simulation results at the 50- and 120-kn off-nominal design points indicated good levels of stability robustness, but indicated the need for suitable controller scheduling strategies to retain adequate performance characteristics over the full flight envelope. Good robustness properties were also observed for designs carried out at other points in the flight envelope; see Ref. 5 for details.

If significant redesign of subcontrollers is to be carried out at subsystem level, then closed-loop performance may deviate significantly from the nominal specifications derived earlier. This fact raises the need to establish robustness specifications for the subcontrollers. Robust stability specifications for the subcontroller K_{ea} can be derived as follows. Writing the closed-loop transfer function matrix from $Z_{\text{ea}\,c}$ to Z_{ea} as a single block Q, variations in the dynamics of this system can be represented by an unstructured additive uncertainty block Δ, as shown in Fig. 9. Using the small gain theorem,[18] a frequency-dependent scalar upper bound on the maximum singular

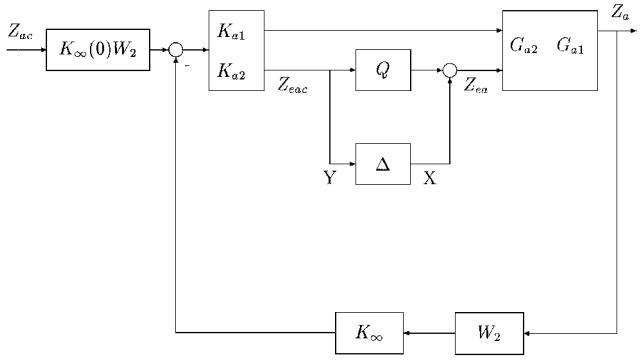

Fig. 9 Extraction of interaction uncertainty.

value of Δ, such that stability of the closed-loop system is preserved, is then given by

$$L(j\omega) = \frac{1}{\bar{\sigma}[M(j\omega)]}$$

where

$$M = -K_{a2}K_\infty W_2\,(I + G_{a1}K_{a1}K_\infty W_2 + G_{a2}QK_{a2}K_\infty W_2)^{-1}\,G_{a2}$$

In the partitioning procedure of the preceding section, the nominal performance specifications generated for the closed-loop engine subsystem were that it must have zero steady-state tracking error and a bandwidth of 30 rad/s. From analysis of the singular values of $L(j\omega)$, the minimum and maximum bandwidths for K_{ea} such that overall closed-loop stability is retained were calculated as 22 and 37 rad/s, respectively. For full independent development of this subcontroller, robust performance specifications would also be required; the work reported in Ref. 6 addresses this issue.

V. Discussion

A centralized approach to the problem of IFPC system design was adopted. Because the centralized controller explicitly takes into account all of the possible interactions between the various subsystems, it can fairly be claimed that it represents a baseline for the optimal achievable performance with a fully integrated system. Alternatively, as argued in Ref. 6, the radically different nature of the flight and propulsion control problems may mean that only detailed separate designs by experts in the relevent areas will deliver truly optimal controllers. From the experience gained in this study, the authors believe that a third viewpoint is possible. This is, that the centralized controller can be regarded as an initial, general design that focuses on satisfying high-level specifications and investigating the effect of subsystem interactions. Subsequent partitioning of the centralized controller can then allow for redesign at subsystem level, subject to satisfaction of the relevent performance and stability specifications. Because the subcontrollers can be designed using any synthesis technique, and subsystem specifications relate only to interface variables and not to internal subsystem variables, substantial freedom exists for detailed redesign at subsystem level even under a centralized approach.

VI. Conclusions

A systematic methodology for IFPC design was presented and applied to the VAAC Harrier IFPC problem. The methodology is based on a centralized approach and uses the method of $\mathcal{H}_\infty$ loop-shaping for controller synthesis. The centralized controller was partitioned into low-order subcontrollers, according to a step by step procedure. Robust stability specifications for the engine subcontroller were derived. Performance properties of the centralized and partitioned IFPC systems were validated via nonlinear simulations.

Acknowledgment

This work was conducted with the support of the U.K. Defence and Evaluation Research Agency through Extramural Research Agreement ASF/2447/U.

References

[1]Tischler, M. B. (ed.), *Advances in Aircraft Flight Control,* Taylor and Francis, London, 1996, Chap. 6, pp. 159–186.

[2]Hyde, R. A., and Glover, K., "Taking $\mathcal{H}^\infty$ Control into Flight," *Proceedings of the 32nd IEEE Conference on Decision and Control* (San Antonio, TX), Inst. of Electrical and Electronics Engineers, New York, 1993, pp. 1458–1463.

[3]Hyde, R. A., *$\mathcal{H}^\infty$ Aerospace Control Design—A VSTOL Flight Application*, Springer–Verlag, London, 1995, pp. 191–199.

[4]Postlethwaite, I., and Bates, D. G., "Integrated Flight and Propulsion Control System Design via $\mathcal{H}^\infty$ Loop-Shaping and Partitioning," *Proceedings of the AIAA Conference on Guidance, Navigation and Control* (Boston, MA), AIAA, Reston, VA, 1998, pp. 989–998.

[5]Postlethwaite, I., and Bates, D. G., "Robust Integrated Flight and Propulsion Control (IFPC) System Design for the Harrier STOVL Aircraft," *Proceedings of the IEE International Conference on Control 98* (Swansea, Wales, UK), Inst. of Electrical Engineers, London, 1998, pp. 1516–1521.

[6]Rock, S. M., Emami-Naeini, A., and Neighbors, K., "Integrated Flight/Propulsion Control: Subsystem Specifications," *Journal of Guidance, Control, and Dynamics*, Vol. 17, No. 1, 1994, pp. 201–208.

[7]Garg, S., Ouzts, P. J., Lorenzo, C. F., and Mattern, D. L., "IMPAC—An Integrated Methodology for Propulsion and Airframe Control," *Proceedings of the American Control Conference* (Boston, MA), Inst. of Electrical and Electronics Engineers, New York, 1991, pp. 755–760.

[8]Garg, S., "Robust Integrated Flight/Propulsion Control Design for a STOVL Aircraft Using $\mathcal{H}^\infty$ Control Design Techniques," *Automatica*, Vol. 29, No. 1, 1993, pp. 129–145.

[9]Garg, S., "Partitioning of Centralized Integrated Flight/Propulsion Control Design for Decentralized Implementation," *IEEE Transactions on Control System Technology*, Vol. AC-1, No. 2, 1993, pp. 93–100.

[10]"Simulink: Dynamic Simulation for MATLAB," User's manual, MathWorks, Natick, MA, 1997.

[11]Franklin, J. A., Stortz, M. W., Borchers, P. F., and Moralez, E., III, "Flight Evaluation of Advanced Controls and Displays for Transition and Landing on the NASA V/STOL Systems Research Aircraft," NASA TP 3607, 1996, pp. 5–8.

[12]Franklin, J. A., "Design Criteria for Integrated Flight/Propulsion Control Systems for STOVL Fighter Aircraft," Piloting Vertical Flight Aircraft: A Conf. on Flying Qualities and Human Factors, San Francisco, CA, 1993, pp. 37–57.

[13]McFarlane, D., and Glover, K., "A Loop Shaping Design Procedure Using $\mathcal{H}^\infty$ Synthesis," *IEEE Transactions on Automatic Control*, Vol. AC-37, No. 6, 1992, pp. 759–769.

[14]Postlethwaite, I., O'Young, S. D., Gu, D. W., and Hope, J., "$\mathcal{H}^\infty$ Control System Design: A Critical Assessment Based on Industrial Applications," *Proceedings of the 10th International Federation of Automatic Control World Congress on Automatic Control* (Munich, Germany), International Federation of Automatic Control, Laxenburg, Austria, Vol. 8, 1987, pp. 328–333.

[15]Postlethwaite, I., Samar, R., Choi, B. W., and Gu, D. W., "A Digital Multi-Mode $\mathcal{H}^\infty$ Controller for the Spey Turbofan Engine," *Proceedings of the 3rd European Control Conference* (Rome, Italy), Vol. 4, European Union Control Association, San Martin d'Hères, France, 1995, pp. 3881–3886.

[16]Skogestad, S., and Postlethwaite, I., *Multivariable Feedback Control*, Wiley, New York, 1996, pp. 5–8.

[17]Samar, R., Postlethwaite, I., and Gu, D. W., "Model Reduction with Balanced Realisations," *International Journal of Control*, Vol. 62, No. 1, 1995, pp. 33–64.

[18]Zames, G., "On the Input–Output Stability of Nonlinear Time-Varying Feedback Systems, Parts I and II," *IEEE Transactions on Automatic Control*, Vol. AC-11, April and July 1966, pp. 228–238 and 465–476.